

Poly(tetraaryllindenofluorene)s: New Stable Blue-Emitting Polymers

Josemon Jacob, Jingying Zhang, Andrew C. Grimsdale, and Klaus Müllen*

Max-Planck-Institute for Polymer Research, Ackermannweg 10, 55128 Mainz, Germany

Martin Gaal and Emil J. W. List

*Christian Doppler Laboratory "Advanced Functional Materials", Institute of Solid State Physics, Graz University of Technology, Petersgasse 16, 8010 Graz, Austria, and Institute of Nanostructured Materials and Photonics, Franz-Pichler-Strasse 30, A-8160 Weiz, Austria**Received June 23, 2003; Revised Manuscript Received August 25, 2003*

ABSTRACT: The problem of long wavelength emission from ketone defects in polyindeno[1,2-b]fluorenes can be overcome by the introduction of aryl substituents which are much less susceptible to oxidation. A new polyindeno[1,2-b]fluorene with octylphenyl side chains has been prepared via a terphenyl intermediate. Unlike alkyl-substituted polyindeno[1,2-b]fluorenes, this displays stable blue emission in the solid state. Blue-emitting LEDs have been fabricated whose emission is stable at voltages below 10 V, with brightnesses of up to 125 cd/m² and efficiencies of up to 0.11 cd/A. Furthermore, no emission from ketone defects was detected even in devices run at voltages above 20 V.

Introduction

Luminescent conjugated polymers are of considerable importance as the active materials in emerging new technologies such as organic light-emitting diodes (LEDs)^{1,2} and polymer lasers.³ One area of major ongoing effort in academic and industrial research into these materials is the development of materials which show efficient, stable blue emission.⁴ Much research into blue-emitting materials has centered on phenylene-based polymers such as polyfluorenes (PFs, **1**),^{5,6} polyindeno[1,2-b]fluorenes (PIFs, **2**),^{7,8} and ladder-type polyphenylenes (LPPPs, **3**) (Figure 1).⁹

All of these materials show blue to blue-green emission in solution, which red-shifts with increasing rigidity of the polymer chain with emission maxima of 420 nm for **1**, 430 nm for **2**, and 450 nm for **3**. In the solid state the appearance of longer wavelength emission bands causes the emission color to become green or yellow.^{5,7–9} The source of this long wavelength emission was initially believed to be excimer emission from aggregates formed by π -stacking of the polymer chains.¹⁰ It has been found that polymers **1** with *n*-alkyl side chains display a unique packing behavior in the condensed phase. For such samples, as well as the regular, glassy (α)-phase, a novel phase, the so-called β -phase, has been identified which shows a distinct red shift of absorption and emission peaks.⁶

Recently, the occurrence of the long wavelength emission band for **1** has been correlated to the emission from ketonic defects incorporated in the polymer backbone as 9-fluorenone units.^{6,11,12} Furthermore, the synthesis of fluorene–fluorenone copolymers with controlled amounts of fluorenone and quantum chemical calculations have established a quantitative correlation between the 9-fluorenone content and the low-energy emission band intensity.¹³ Thus, the evidence favors the main source of the long wavelength emission in polyfluorenes (**1**) being from ketone defects. It has also been proposed that the yellow emission seen from LPPP (**3**) arises from ketonic defect sites.¹⁴

For PIFs (**2**) the long wavelength emission band appears in the green around 565 nm. We have shown that the amount of green emission seen from PIFs (**2**) correlates with the degree of π -stacking shown by the detection of fibrillar structures in the film morphologies by atomic force microscopy (AFM) and with the proportion of *n*-alkyl side chains on the polymers.⁸ Thus, a polymer **2a** with all *n*-alkyl side chains showed green solid-state photoluminescence (PL) and electroluminescence (EL), while a polymer **2b** with branched alkyl side chains initially produced blue EL, but the emission rapidly red-shifted. Copolymers showed intermediate behavior.

Given the similarity of the structures and of the observed phase-forming and optical behavior of PIFs and PFs with the same types of alkyl substituents, it is likely that the long-wavelength emission in PIFs stems from similar sources to that in PFs. Moreover, delayed PL measurements in solution show the presence of an emission band at 545 nm,¹⁵ which is intermediate between the positions of the corresponding defect emission bands seen for PFs (**1**) and LPPPs (**3**), as would be expected for defect emission from a PIF. This suggests that the long wavelength emission band in polyindeno[1,2-b]fluorenes also arises from emission from ketone defect sites. We currently believe the evidence favors emission from ketone defects as being the most probable source of the long wavelength emission in PIFs, and investigations are underway to test this, the results of which will be published separately.

We have previously demonstrated that stable blue EL can be obtained from polyfluorenes with bulky dendrimer **4**¹⁶ or triphenylamine **5**¹⁷ side chains (Figure 2). The stability of the blue emission from polymers **4** and **5** arises from their greater resistance to oxidation and a reduction in excimer diffusion to any ketone defect sites that might form. It has been shown that exciton diffusion is affected by the dendrimer side chains in the stable blue-emitting polyfluorene **4**.¹⁸

From the above results it can be seen that polyindeno[1,2-b]fluorenes **6** with aryl substituents would be expected to show stabler blue emission than the alkyl-substituted polymers **2**. In this paper we report the

* To whom correspondence should be addressed: Fax +49 6131 379350; e-mail muellen@mpip-mainz.mpg.de.

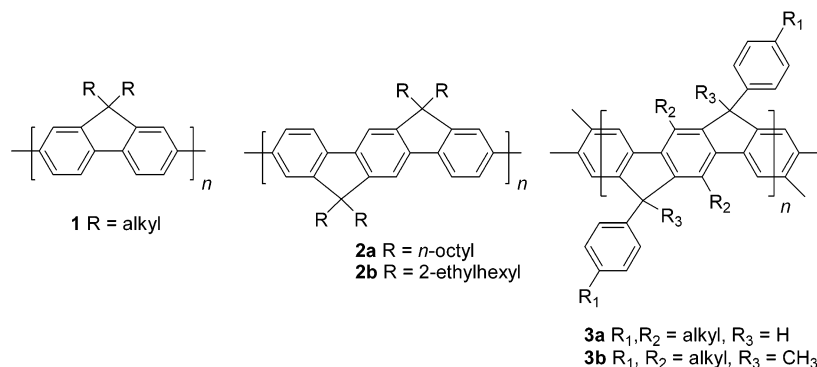


Figure 1. Typical blue-emitting conjugated polymers.

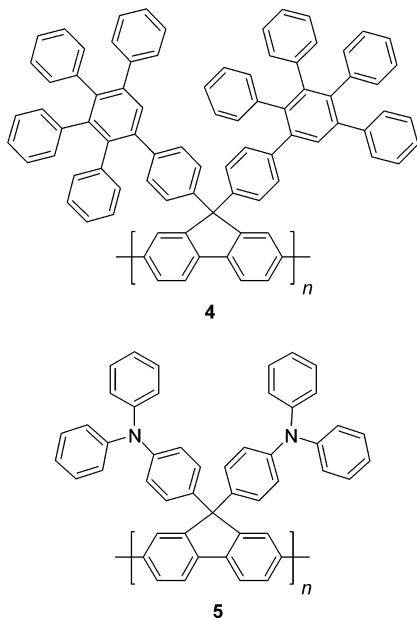


Figure 2. Stable blue-emitting polyfluorenes.

synthesis of poly(tetraaryllindenofluorene)s and their emission properties.

Results and Discussion

As aryl substituents cannot be attached directly to indenofluorene, an indirect synthesis of the desired monomers—2,8-dibromo-6,6,12,12-tetraaryllindenofluorene (**7**)—was needed. In such a synthetic route the five-membered rings would be prepared by ring closure of a terphenyl **8** with two diarylmethanol substituents. Such methods have been used in the synthesis of LPPP (**3**)⁹ and of the monomer of the dendronized polyfluorene (**4**).^{16a} As bromination of indenofluorenes is difficult to control so as to get only substitution at the 2- and 8-positions,⁶ we decided to use the electrophilic displacement of a trimethylsilyl group with bromine at these positions to introduce the bromines without danger of overbromination. The key intermediate for the synthesis of the desired monomers **7** was therefore the bis(trimethylsilyl)terphenyl **9**. Addition of 4 equiv of an aryllithium followed by conversion of the trimethylsilyl groups to bromines was expected to give **7** in good yield. The synthesis thus devised of the polymers **6** is shown in Scheme 1.

Suzuki coupling of dimethyl 2,5-dibromoterephthalate (**10**)¹⁹ with 4-(trimethylsilyl)benzeneboronic acid (**11**) proceeded smoothly to give the terphenyl **9** in 92% yield. Addition of 4 equiv of aryllithium in dry THF at

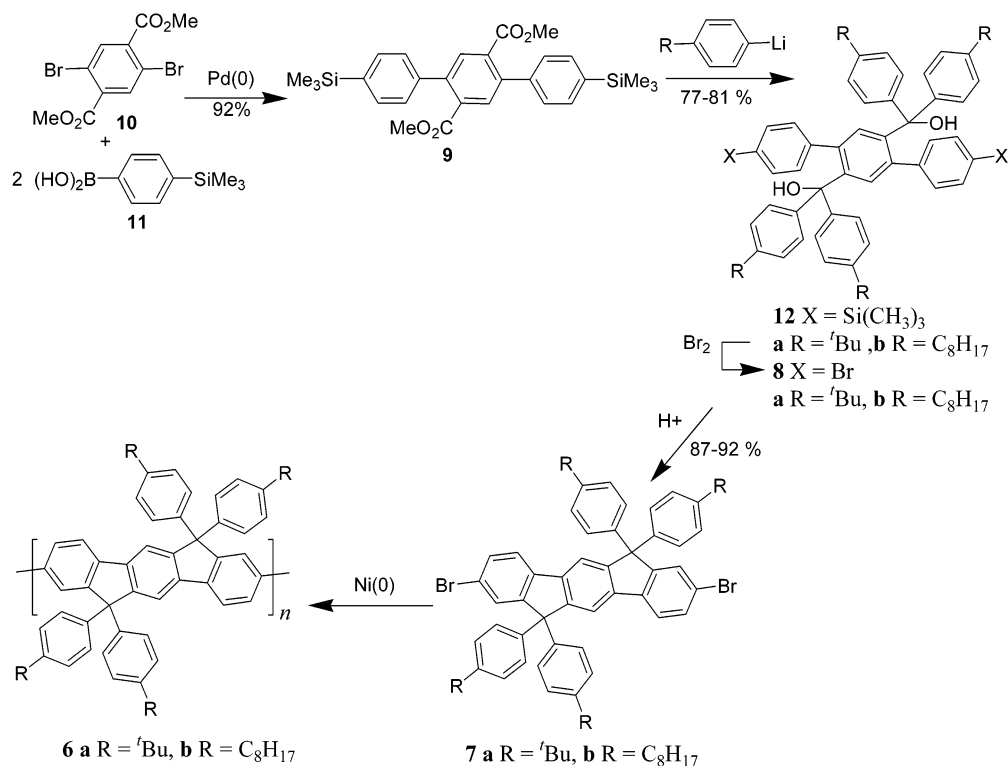
−78 °C gave the diol **12** in 77–81% yield. Displacement of the silyl groups with bromine and sodium acetate followed by ring closure of **8** with concentrated sulfuric acid in hot acetic acid then gave the desired monomers **7** in 87–92% yield (71% overall). These were then polymerized with bis(cycloocta-1,7-diene)nickel(0) and 2,2′-bipyridine in toluene–DMF to give the polymers **6**.

The *tert*-butyl substituent in **7a** was found to be too poor a solubilizing group to retain the growing polymer chain of **6a** in the reaction medium, so that the product was determined to be a mixture of oligomers by GPC ($M_n = 1940$, $M_w = 3470$), but the octylphenyl groups in **7b** allowed formation of a high molar mass polymer **6b** ($M_n = 66\,400$, $M_w = 257\,000$). These GPC results were obtained using polyphenylene standards²⁰ which are much closer in structure to the rigid-rod polymers **6** than the polystyrene standards commonly used for GPC calibration and therefore can be expected to give more accurate mass values. This corresponds to a degree of polymerization of about 66 units (ca. 200 benzene rings).

The absorption and emission spectra for polymer **6b** are shown in Figure 3. The absorption was strong in the violet with the maximum at 417 nm. The PL was blue both in solution ($\lambda_{\max} = 428$ nm) and as a thin film ($\lambda_{\max} = 434$ nm) (Figure 3). The small Stokes shift of only 11 nm indicates the rigidity of the polymer. The emission from the oligomeric **6a** was only slightly blue-shifted (~1 nm) compared with the polymer **6b** as the oligomers were close to the effective conjugation length previously determined for PIFs ($n = 5$).⁶ The solid-state PL spectra of **6b** closely resembles that of the ethylhexyl polymer **2b** with two peaks at 434 and 457 nm and a small shoulder at about 515 nm. No sign of the broad green emission band at 560 nm seen for the tetraoctyl polymer **2a** was observed.

Photoinduced Absorption and Electroluminescence Measurements on Polymer 6b. Figure 4 shows the absorbance and PL emission spectra for polymer **6b** in the solid state. The PL and absorption spectra are very similar to the spectra observed in solution, however, exhibiting a bathochromic shift of a ca. 60 meV. The PIA spectrum (Figure 4) is characterized by one broad feature with a maximum at ca. 810 nm. From a comparison to various polyfluorene derivatives this band is assigned to a transition from the lower to a higher lying triplet state (T_1 – T_n absorption). Note that this band is similar to the triplet PIA of polymer **3b**.

LEDs were constructed with structure ITO/PEDOT:PSS (80 nm)/**6b**/Ca (50 nm)/Al(200 nm). The thickness of the active layer was varied by varying the concentration of the polymer **6b** in toluene used for spin-coating. A solution of 5 g/L gave films of 70–80 nm thickness,

Scheme 1. Synthesis of Poly(6,6,12,12-tetraaryllindenofluorene)s **6**

while a solution of 10 g/L produced films of 150 nm. LEDs made using the thicker films required operating voltages above 10 V, while for the devices with thinner films the emission onset was at 5 V. The emission from all devices had maxima in the blue at 435 and 455 nm with a long tail into the red (Figure 5).

The emission from the devices with a 70 nm thick layer of **6b** showed a pure blue emission (Figure 6), with a maximum luminance of 125 cd/m² and an efficiency of 0.11 cd/A for the best devices tested. The long wavelength emission from devices with thicker emissive layers was more intense due to greater self-absorption within the thicker layer, with a maximum luminance of up to 108 cd/m² and an efficiency of up to 0.11 cd/A.

The stability of the blue emission was found to be dependent upon the driving current of the device. The devices with 70 nm thick emissive layers were stable below 50 mA/cm² at ca. 7 V bias and showed no significant degradation when operated over 10–15 min

under argon. By contrast, the devices operated at higher bias voltages with driving current densities of 0.5–1.0 A/cm² showed an increase in emission from the long

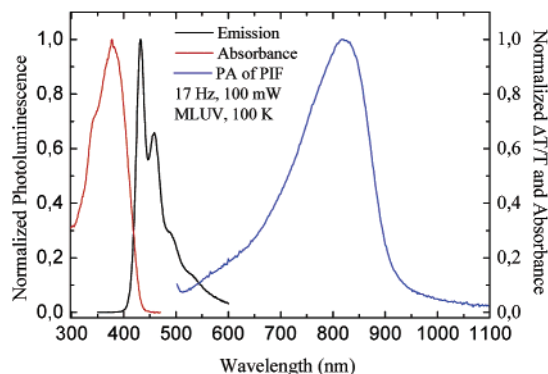


Figure 4. PL emission (black) and excitation (red) spectra for a film of polymer **6b** at 300 K together with the photo-induced absorption spectrum (blue) of **6b** at 77 K (laser excitation at 351 and 363 nm).

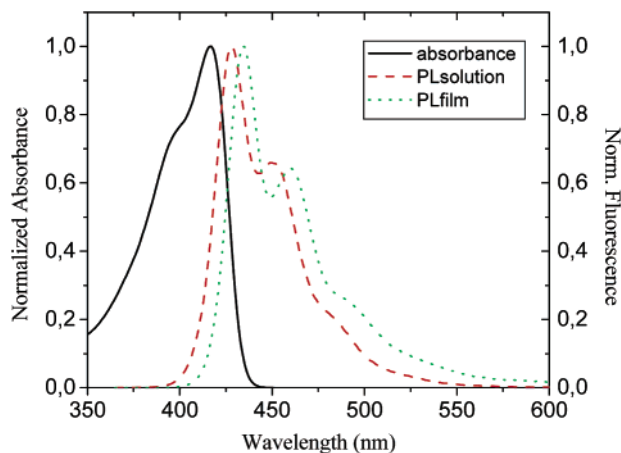


Figure 3. Absorption (solid) and PL emission in solution (dashed) and thin film (dots) of **6b**.

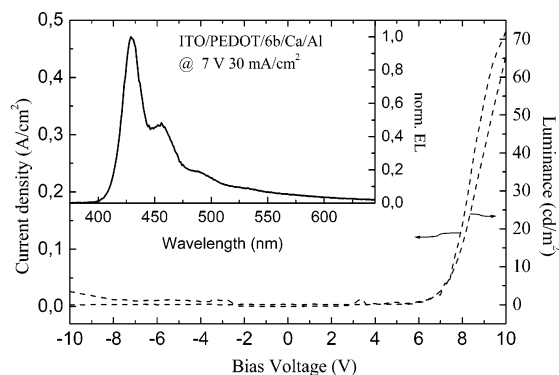


Figure 5. EL emission spectrum and current–voltage and luminance–voltage graphs for device ITO/PEDOT:PSS/**6b**(70 nm)/Ca/Al.

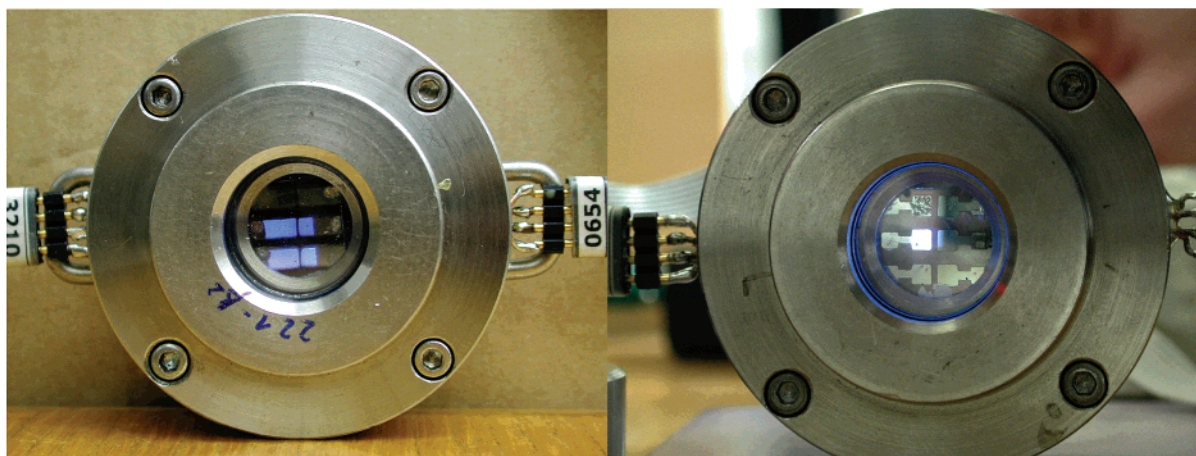


Figure 6. Emission from devices operated at 7 V (left) and 16 V (right). The whitish color of the latter is due to saturation of the CCD camera at high intensities.

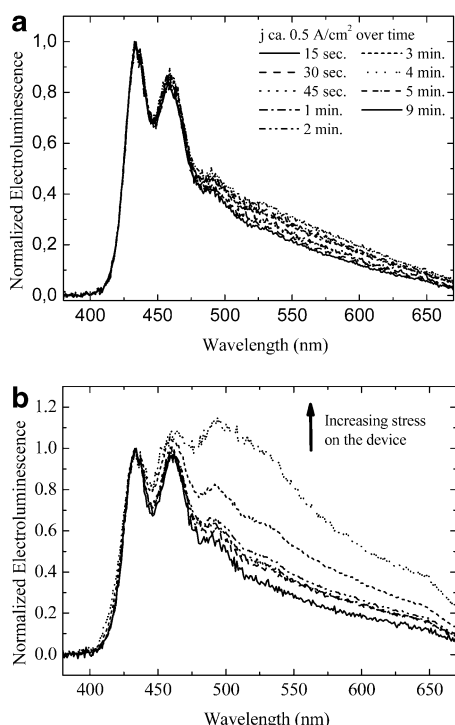


Figure 7. (a) EL emission from device ITO/PEDOT:PSS/6b (150 nm)/Ca/al at 16 V and $j < 0.5 \text{ A/cm}^2$ over time. (b) EL emission from same device driving current densities between 0.5 and 1 A/cm^2 (19 and 25 V).

wavelength tail between 500 and 650 nm when operated for several minutes (Figure 7). This is dissimilar to the change in emission seen for the dendronized polyfluorene **4** when run in continuous mode for extended periods as no clear peak around 520–550 nm appears.^{15b} Increasing the bias in these devices between 19 and 25 V led to a marked increase in an emission band at 500 nm, but again with no sign of a new band as would be seen from the formation of a ketone defect due to oxidation of the bulk polymer. Above 25 V the devices melted. The green emission band at 565 nm seen for polyindenofluorenes **2**,⁸ which we propose is due to the formation of ketone defects analogous to those produced upon in polyfluorenes **1**, was not observed for any device using **6b**. This suggests that **6b** is much more resistant to oxidation than **2**.

Though some further optimization of devices is required to obtain higher brightness and efficiency, it is

clear from these results that poly(tetraarylindenofluorene)s are extremely promising materials for stable blue emission in LEDs. More recent detailed device studies on PF and PIF based devices have revealed that the long wavelength tail between 500 and 650 nm may stem from defects induced by the deposition of the metal cathodes as also suggested by the Santa Barbara group.¹¹ However this mechanism is not correlated with the formation of oxidation-related emissive bulk defects, i.e., keto-type defects, but only with the conditions under which the cathode is deposited. Such defects cannot be overcome by a synthetic strategy as presented here, but can only be avoided by choosing proper interface layers to protect the polymer during deposition of the cathode metal.¹¹ Identifying the exact nature of this defect as well as testing and optimizing such protection layers which may simultaneously act as electron transport layers will be the subject of further studies.

Conclusions

Polyindenofluorenes with aryl substituents on the methine bridges have been prepared in high yields by a short, efficient synthetic route. These polymers, unlike previous indenofluorene-based polymers, show stable blue PL and EL emission. Efficient, stable blue-emitting LEDs have been fabricated using the polymer **6b**. The improved stability is attributed to the greater resistance of the polymers to oxidation.

Experimental Section

Materials and Methods. Commercial grade reagents were used without further purification. Solvents were purified and dried using standard procedures. 4-Octylbromobenzene and 4-trimethylsilylbenzeneboronic acid were purchased from commercial sources and used as received. ¹H and ¹³C NMR spectra were recorded in CDCl₃ on a Bruker DRX-250 spectrometer. GPC measurements used PL-gel columns (three columns, 10 μm gel, pore widths: 500, 10⁴, and 10⁵ Å) connected with ultraviolet/visible (UV/vis) detectors. UV-vis transmission spectra were measured using a Perkin-Elmer Lambda9 spectrophotometer. PL emission and excitation spectra were recorded using a Shimadzu RF5301 spectrofluorometer or a SPEX Fluorolog 2 type 212 spectrometer.

The ITO-covered glass substrates for the PLEDs were thoroughly cleaned in a variety of organic solvents and exposed to an oxygen plasma dry cleaning step. PEDOT:PSS (Baytron P from Bayer Inc.) layers were spin-coated under ambient conditions and dried according to specifications by Bayer Inc. under inert atmosphere. The emissive polymer films were spin-

cast from solution and dried at 80 °C overnight in vacuo. Metal electrodes were thermally deposited in a Balzers MED010 vacuum coating unit at base pressures of below 2×10^{-6} mbar.

EL spectra were recorded using an ORIEL spectrometer with an attached CCD camera. The current/luminance/voltage (ILV) characteristics were recorded in a customized setup using a Keithley 236 source measure unit for recording the current/voltage characteristics while recording the luminance using a calibrated photodiode attached to an integrating sphere (Ulbrich).

For PIA measurements the sample was excited with the 351 and 363 nm pump beam of the Ar⁺ laser (100 mW), which was mechanically chopped at 17 Hz, providing the reference for the lock-in amplifier. The sample was mounted in an optically accessible cryostat under a dynamic vacuum of less than 10^{-5} mbar to prevent photooxidation. A 200 W halogen lamp provided the source for the transmission measurement. All PA spectra were measured at 77 K and were corrected for the PL and optical throughput of the setup.

Synthesis of the Triphenylene Diester, 9. To 1.50 g of the dibromo diester **10**¹⁷ (4.26 mmol) in a 100 mL flask, 2.07 g of 4-(trimethylsilyl)benzeneboronic acid (**11**) (2.5 equiv) was added followed by 1.77 g of K₂CO₃, 30 mL of toluene, and 15 mL of water. The flask was purged with argon for 15 min, and then 197 mg of (Ph₃P)₄Pd was added and the mixture was heated with stirring at 70 °C in an oil bath for 24 h when TLC analysis showed complete consumption of **11**. The crude reaction mixture was extracted with toluene, and the extract was concentrated and chromatographed on silica using 2–30% ethyl acetate in hexane as eluent. The product was isolated as a white solid. Yield = 1.91 g (92%). Melting point = 212–213 °C. Elemental analysis: Calcd: C, 68.53; H, 6.98%. Found: C, 68.08; H, 7.17%. ¹H NMR (CDCl₃): δ 7.85 (s, 2H) 7.64 (d, J = 8.0 Hz, 4H) 7.39 (d, J = 8.0 Hz, 4H) 3.73 (s, 6H) 0.36 (s, 18H). ¹³C NMR: δ 169.38, 142.41, 141.63, 141.29, 134.66, 134.62, 133.43, 129.08, 53.53, –1.23.

Synthesis of the Diols 12. To 1.47 mL of 4-octylbromobenzene (6 mmol) in 75 mL of dry THF cooled to –78 °C in an acetone/dry ice bath, 3.95 mL of *n*-butyllithium (1.6 M, 6.3 mmol) was added dropwise with stirring. After 20 min, 0.50 g of **9** (1 mmol) dissolved in 20 mL of THF was added dropwise; the mixture was allowed to slowly warm to room temperature over 14 h, and then the reaction was quenched with brine. The crude product was extracted into ether, and the extract was washed with brine and dried. Removal of solvent followed by recrystallization from hexane gave **12b** as a white solid (975 mg, 81%). Melting point = 177–178 °C. Elemental analysis: Calcd: C, 82.91; H, 9.67%. Found: C, 82.86; H, 9.61%. FDMS m/z = 1186.6. ¹H NMR (CD₂Cl₂): δ 7.23 (d, J = 7.9 Hz, 4H) 7.07 (m, 16H) 6.72 (d, J = 7.9 Hz, 4H) 6.60 (s, 2H) 2.84 (s, 2H) 2.60 (t, J = 7.3 Hz, 8H) 1.61 (m, 8H) 1.31 (m, 40H) 0.89 (t, J = 7.0 Hz, 12H) 0.23 (s, 18H). ¹³C NMR: δ 145.28, 144.31, 142.78, 142.31, 139.68, 139.15, 134.45, 133.22, 128.99, 128.19, 128.13, 83.23, 35.82, 32.34, 31.89, 29.90, 29.72, 29.65, 23.10, 14.30, –1.10.

Diol **12a** was prepared as a white solid in 77% yield by addition of 4-*tert*-butylphenyllithium to **9** under the same conditions. Elemental analysis: Calcd: C, 82.77; H, 8.58%. Found: C, 81.87; H, 8.53%. FDMS m/z 963.70. ¹H NMR: δ 7.26 (d, J = 8.5 Hz, 8H) 7.18 (d, J = 8.2 Hz, 4H) 7.06 (d, J = 8.5 Hz, 8H) 6.69 (d, J = 8.2 Hz, 4H) 6.60 (s, 2H) 2.85 (br s, 2H) 1.29 (s, 36H) 0.32 (s, 18H). The solubility was too poor for ¹³C NMR.

Synthesis of the Monomers 7. To 0.88 g of **12b** (0.74 mmol) dissolved in 12 mL of THF, 128.0 mg of sodium acetate (2 equiv) was added, and the mixture was cooled to 0 °C. To this, 0.16 mL of bromine (4.2 equiv) was added, and the mixture was stirred for 20 min. Then, 0.87 mL of triethylamine (8 equiv) was added followed by aqueous sodium sulfite solution. The crude **8b** obtained after extraction with dichloromethane was used without further purification for the next step.

The crude **8b** was added to 20 mL of glacial acetic acid containing 3 drops of H₂SO₄ and heated at 90 °C for 3 h. The mixture was cooled, and the product was extracted into

dichloromethane. The extract was washed with sodium bicarbonate solution, dried, and then concentrated. The residue was purified by chromatography on silica using 0–2% ethyl acetate in hexane as eluent to give **7b** as a white solid (751 mg, 87%). Elemental analysis: Calcd: C, 78.33; H, 7.96%. Found: C, 77.89; H, 7.79%. FDMS m/z = 1166.9. ¹H NMR (CD₂Cl₂): δ 7.73 (s, 2H) 7.49 (m, 6H) 7.10 (m, 16H) 2.56 (t, J = 8.5 Hz, 8H) 1.58 (m, 8H) 1.28 (m, 40H) 0.88 (t, J = 8.5 Hz, 12H). ¹³C NMR: δ 154.84, 152.26, 143.10, 142.68, 140.13, 139.70, 131.35, 129.96, 129.20, 128.70, 122.44, 122.00, 118.63, 65.57, 36.24, 32.66, 32.25, 30.23, 30.20, 30.01, 23.45, 14.65.

Monomer **7a** was prepared from diol **12a** as a white solid in 92% yield by the same procedure. Elemental analysis: Calcd: C, 76.59; H, 6.43%. Found: C, 76.61; H, 6.43%. FDMS m/z 940.60. ¹H NMR: δ 7.66 (s, 2H) 7.48 (m, 2H) 7.41 (m, 4H) 7.21 (d, J = 8.5 Hz, 8H) 7.05 (d, J = 8.5 Hz, 8H) 1.28 (s, 36H). The solubility was too poor for ¹³C NMR.

Synthesis of Poly(tetraarylindenofluorene)s 6. 397 mg of bis(cyclooctadiene)nickel(0) (1.44 mmol), 225 mg of 2,2'-bipyridine (1.44 mmol), and 0.18 mL of cyclooctadiene (1.47 mmol) were added to a Schlenk flask containing 6 mL of toluene and 6 mL of DMF in a glovebox. The resulting solution was heated under an argon atmosphere for 30 min at 60 °C in an oil bath, and then 700 mg of the monomer **7b** (0.6 mmol) was added dropwise. The mixture was heated at 95 °C for 4 days; then 0.1 mL of bromobenzene was added, and the reaction continued for a further 12 h. The solution was poured into 300 mL of 1:1 concentrated hydrochloric acid and methanol and stirred for 4 h. The solution was extracted with 500 mL of toluene, and the crude polymer **6b** obtained on removal of solvent was redissolved in 50 mL of THF. Reprecipitation from methanol gave 595 mg of polymer **6b** after drying (98% yield). GPC (THF, PPP standards): M_n = 6.64×10^4 g/mol, M_w = 2.57×10^5 g/mol; D = 3.86. Elemental analysis: Calcd: C, 90.79; H, 9.22%. Found: C, 90.60; H, 9.36%. ¹H NMR: δ 7.49 (br, 6H) 7.05 (br, 18H) 2.52 (br, 8H) 1.37 (br, 44H) 0.98 (br, 16H).

Polymer **6a** was obtained from monomer **7a** in 78% yield by the same procedure. GPC (THF, PPP standards): M_n = 1.94×10^3 g/mol, M_w = 3.74×10^3 g/mol; D = 1.73.

Acknowledgment. We acknowledge the financial support of the Bundesministerium für Bildung und Forschung (Projects 13N8165 OLAS and 13N8215 OLED). J.J. acknowledges the Alexander von Humboldt Stiftung for the grant of a Research Fellowship. The CDL-AFM is a key member of the long-term AT&S research strategies.

References and Notes

- (1) Kraft, A.; Grimsdale, A. C.; Homes, A. B. *Angew. Chem., Int. Ed.* **1998**, *37*, 402.
- (2) Mitschke, U.; Bäuerle, P. *J. Mater. Chem.* **2002**, *10*, 1471.
- (3) McGehee, M. D.; Heeger, A. J. *Adv. Mater.* **2000**, *12*, 1655.
- (4) Kim, D. Y.; Cho, H. N.; Kim, C. Y. *Prog. Polym. Sci.* **2000**, *25*, 1089.
- (5) Neher, D. *Macromol. Rapid Commun.* **2001**, *22*, 1365.
- (6) Scherf, U.; List, E. J. W. *Adv. Mater.* **2002**, *14*, 477.
- (7) Setayesh, S.; Marsitzky, D.; Müllen, K. *Macromolecules* **2000**, *33*, 2016.
- (8) Grimsdale, A. C.; Leclère, Ph.; Lazzaroni, R.; Mackenzie, J. D.; Murphy, C.; Setayesh, S.; Silva, C.; Friend, R. H.; Müllen, K. *Adv. Funct. Mater.* **2002**, *12*, 729.
- (9) Reviewed in: Scherf, U. *J. Mater. Chem.* **1999**, *9*, 1853.
- (10) (a) Lemmer, U.; Heun, S.; Mahrt, R. F.; Scherf, U.; Hopmeier, M.; Siegner, U.; Göbel, E. O.; Müllen, K.; Bässler, H. *Chem. Phys. Lett.* **1995**, *240*, 373. (b) Pannozzo, S.; Vial, J.-C.; Kervalla, Y.; Stéphan, O. *J. Appl. Phys.* **2002**, *92*, 3495. (c) Herz, L. M.; Phillips, R. T. *Phys. Rev. B* **2000**, *61*, 13691. (d) Zeng, G.; Yu, W. L.; Chua, S. J.; Huang, W. *Macromolecules* **2002**, *35*, 6907.
- (11) Gong, X.; Iyer, P. K.; Moses, D.; Bazan, G. C.; Heeger, A. J.; Xiao, S. S. *Adv. Funct. Mater.* **2003**, *13*, 325.

- (12) (a) List, E. J. W.; Günter, R.; Scandiucci de Freitas, P.; Scherf, U. *Adv. Mater.* **2002**, *14*, 374. (b) Gaal, M.; List, E. J. W.; Scherf, U. *Macromolecules* **2003**, *36*, 4236.
- (13) (a) Scandiucci de Freitas, P.; Scherf, U.; Collon, M.; List, E. J. W. *e-Polym.* **2002**, No. 0009. (b) Zojer, E.; Pogantsch, A.; Hennebicq, E.; Beljonne, D.; Brédas, J. L. Scandiucci de Freitas, P.; Scherf, U.; List, E. J. W. *J. Chem. Phys.* **2002**, *117*, 6794. (c) Romaner, L.; Pogantsch, A.; Scandiucci de Freitas, P.; Scherf, U.; Gaal, M.; Zojer, E.; List, E. J. W. *Adv. Funct. Mater.* **2003**, *13*, 597.
- (14) Lupton, J. M. *Chem. Phys. Lett.* **2002**, *365*, 366.
- (15) Keivanidis, P. E.; Lupton, J. M.; Grimsdale, A. C.; Müllen, K., unpublished results. Measurements were carried out by the same method used in ref 18b.
- (16) (a) Setayesh, S.; Grimsdale, A. C.; Weil, T.; Enkelmann, V.; Müllen, K.; Meghdadi, F.; List, E. J. W.; Leising, G. *J. Am. Chem. Soc.* **2001**, *123*, 946. (b) Pogantsch, A.; Wenzl, F. P.; List, E. J. W.; Grimsdale, A. C.; Müllen, K.; Leising, G. *Adv. Mater.* **2002**, *14*, 1061.
- (17) Ego, C.; Grimsdale, A. C.; Uckert, F.; Yu, G.; Srdanov, G.; Müllen, K. *Adv. Mater.* **2002**, *14*, 809.
- (18) (a) List, E. J. W.; Pogantsch, A.; Wenzl, F. P.; Kim, C.-H.; Shinar, J.; Loi, M. A.; Bongiovanni, G.; Mura, A.; Setayesh, S.; Grimsdale, A. C.; Nothofer, H. G.; Müllen, K.; Scherf, U.; Leising, G. *Mater. Res. Soc. Symp. Proc.* **2001**, *665*, C5.47.1. (b) Lupton, J. M.; Schouwink, P.; Keivanidis, P. E.; Grimsdale, A. C.; Müllen, K. *Adv. Funct. Mater.* **2003**, *13*, 154.
- (19) Lambda, J. J. S.; Tour, J. M. *J. Am. Chem. Soc.* **1994**, *116*, 11723.
- (20) Vanhee, S.; Rulkens, R.; Lehmann, U.; Rosenauer, C.; Schulze, M.; Köhler, W.; Wegner, G. *Macromolecules* **1996**, *29*, 5136.

MA034849M